

## QUANTITATIVE NON-RESONANT POSTIONIZATION EXPERIMENTS WITH FEMTOSECOND LASER PULSES

Teiichiro Kono<sup>a</sup>, Vasil Vorsa<sup>b</sup>, Shixin Sun<sup>b</sup> and Nicholas Winograd<sup>b</sup>  
<sup>ab</sup>184 Materials Research Institute Building, University Park 16802 USA  
<sup>a</sup>2-1 Samejima, Fuji, Shizuoka, 416 Japan  
a8911363@ut.asahi-kasei.co.jp

### 1. Introduction

Nonresonant postionization of sputtered neutral atoms offers the possibility of detecting most elements in the periodic table with similar sensitivity and with reduced matrix effects. However, to obtain quantitative data, the photoionization step must be saturated. Ti:Sapphire-based lasers produce a very high power density of pulses and are considered to

be the most likely candidate for that purpose. Even with the power of these systems the laser still needs to be focused to attain saturation. In this case it is difficult to ionize all of the particles in the sputtered plume.

The calculated ionization probabilities for different elements along the radius of a gaussian laser beam are shown in Figure 1. In this scenario, the elements display an intensity disparity due to the variation of the ionization volume. It is apparent that some coefficient such as the relative sensitivity factor needs to be introduced. One way to correct for this difference is to obtain the ratio of the signal intensity to the sample concentration for each element. However the concentration of each species in the postionization volume does not

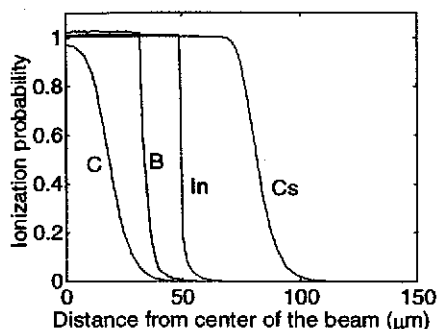


Fig. 1. Ionization probabilities along the radius of a gaussian beam for different elements. See Eq. 1-4.

necessarily reflect the concentration in the sample. Another way is to measure the ionization cross section. Once you obtain the ionization cross section ( $\sigma$ ), it is possible to calculate the concentration from the signal intensity and the laser beam profile.

### 2. Experimental

Time of Flight SIMS equipped with a Ga<sup>+</sup> ion source in conjunction with the Ti:Sapphire laser system [1] was used for all the postionization experiments. The Ti:Sapphire laser system produces pulse energies of 3.3 mJ, 1.2 mJ, 400 uJ and 45 uJ with pulse widths of 100 fs, 150 fs, 200 fs and 300 fs for 800 nm, 400 nm, 267 nm and 200 nm wavelengths, respectively. The focused laser beam profile was measured by a microscopic objective and a CCD camera. The beam power was attenuated through reflections by optical wedges and a combination of a waveplate and a polarizer.

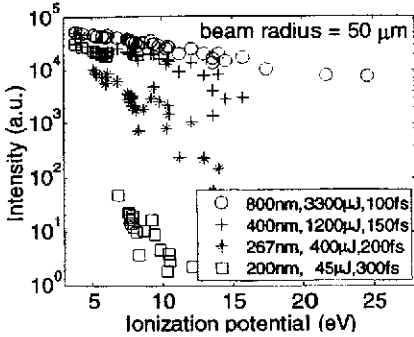


Fig. 2. Calculation results of ion intensities for representative elements plotted against ionization potential.  $\circ$ : 800 nm,  $+$ : 400 nm,  $*$ : 267 nm,  $\square$ : 200 nm. Gaussian beam was used for calculation. See Eq. 1 and 2.

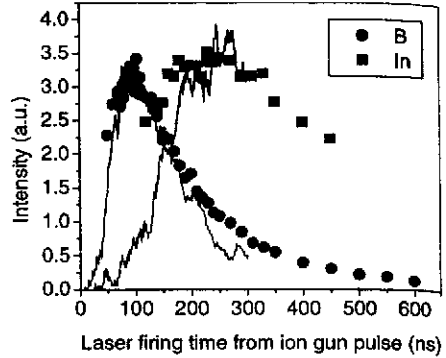


Fig. 3. Intensity vs time difference between laser pulse and ion pulse.  $\bullet$ ,  $\blacksquare$ : Experiment, —: simulation. The primary ion pulse width was fixed at 40 ns.

Since our system produces four different wavelengths, the choice of wavelength for quantitative analysis purposes is of interest. It could be estimated by calculating  $\sigma$  obtained from theoretical calculations [2]. Results from these calculations are shown in Figure 2. The most favorable wavelength for quantitative analysis is 800 nm due to the relatively weak dependence on ionization potential.

Because of the variation in the energy distribution of sputtered neutrals for different elements, the time sequence of laser pulse, ion pulse and extraction voltage as well as the length of the primary ion pulse play important roles in quantitative analysis. The change in the intensities for B and In when changing the laser pulse timing with respect to

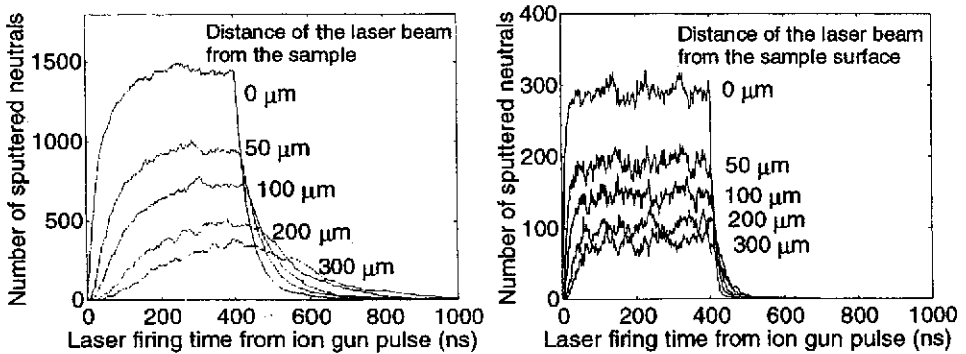


Fig. 4. The calculated number of sputtered neutrals inside the photoionization volume (60  $\mu$ m in radius) for 400 ns ion pulse width plotted against laser firing time from ion gun pulse. Right: Boron, left: Indium.

the ion pulse timing is shown in Figure 3. These elements show different maxima which would lead to errors in quantitation. To avoid this situation, we increase the pulse width up to 400 ns and fire the laser pulse before the end of the ion gun pulse. As shown in Figure 4 the distance of the laser beam from the surface also affects quantitation. The smaller the distance, the better the quantitation. However, even when firing the laser beam at the maximum point for both elements, there still exist large differences in the number of neutrals in the postionization volume, especially when the laser beam size is small as shown in Figure 4. Nevertheless, since the energy distribution is not strongly dependent on the matrix, once the ratio of the neutrals inside the postionization volume to all the neutrals is measured for a standard sample, the concentration in the postionization volume can be converted to the one in the sample by multiplying these factors.

### 3. Measurement of ionization cross section

The calculation model to obtain the ionization cross section used here is based on the following formulas[2-5].

$$N_i = N_0 \iiint \max(P_{MPI}(x, y, z), P_{TI}(x, y, z), P_{BSI}(x, y, z)) dx dy dz \quad (1)$$

$$P_{MPI}(x, y, z) = 1 - \exp\left(-\sigma_k \int F^k(x, y, z, t) dt\right) \quad (2)$$

$$P_{TI}(x, y, z) = \left(\frac{3e}{\pi}\right)^{\frac{3}{2}} \frac{Z^2 (2l+1)}{3n^3 2n-1} \iint \left(\frac{4eZ^3}{(2n-1)n^3 F(x, y, z, t)}\right)^{2n-\frac{3}{2}} \exp\left(-\frac{2Z^3}{3n^3 F(x, y, z, t)}\right) dt \quad (3)$$

$$P_{BSI}(x, y, z) = \begin{cases} 1 & \max(F(x, y, z, t)) \geq F_{BSI} \\ 0 & \max(F(x, y, z, t)) < F_{BSI} \end{cases} \quad F_{BSI} = \frac{\epsilon_0^2 h^2 c E^2}{e^3 m_e a_0 Z} \quad (4)$$

where  $N_i$  is the number of ions created by the laser pulse,  $N_0$  is the initial number of neutrals per unit volume, and  $P_{MPI}$ ,  $P_{TI}$ ,  $P_{BSI}$  are ionization probabilities for multiphoton ionization, tunnel ionization and barrier suppression ionization respectively.  $F$  is the field strength of light which is a function of time and position,  $k$  is the number of photons necessary for ionization and  $\sigma_k$  is the  $k$  photon order ionization cross section.  $Z$  is the multiplicity of ion, and  $l$  and  $n$  are principal and orbital quantum numbers.

To verify the model, power dependence measurements were carried out for several elements. The results for Xe are shown in Figure 5. We report pulse energy instead of power density because of difficulty in defining the power density for a non-gaussian beam. The result yields  $\sigma_3=10^{-79.5} / \text{cm}^6 \text{s}^2$ . Using this approach, the fit value of  $\sigma$  is found to be independent of beam profile.

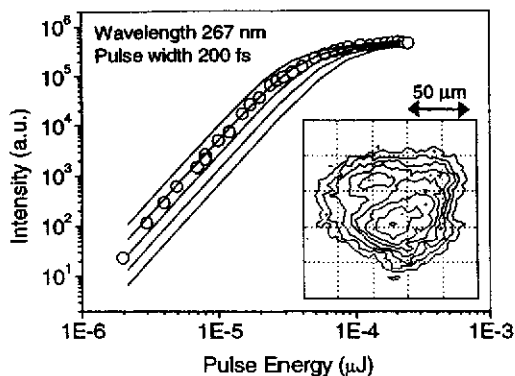


Fig. 5. Signal intensity of Xe vs pulse energy. o:experiment, line:calculation with  $-\log(\sigma_3) = 79.2, 79.5, 79.8, 80.1, 80.4$  from top. The inset shows the measured beam profile used in this measurement and calculation.

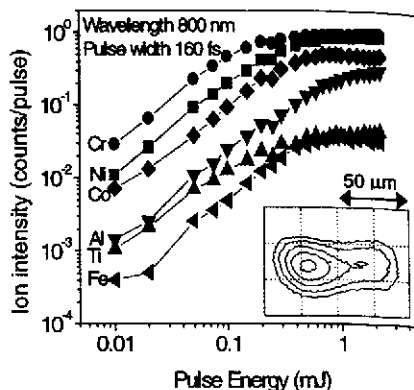


Fig. 6. Pulse energy dependence curves for elements in the stainless steel. The inset shows the measured beam profile used in this measurement and calculation.

Using this method we examined a stainless steel reference sample obtained from NIST. The sample was ion-etched in the spectrometer to remove surface impurities. The power dependence curve is shown in Figure 6. Up to 1 mJ all elements show the same slope of 1.3 which means the ionization for all elements is saturated. The leveling off observed in the high pulse energy region is due to the onset of multiply charged ions and the saturation in detection system. The intensity ratio of Ni, Cr, Ti, Al, Co and Fe at 0.1 mJ were 25.0, 58.2, 1.6, 3.1, 11.6, 0.7 respectively whereas the composition ratio provided by NIST is 52.2, 23.6, 3.6, 3.5, 16.1, 0.97. If the concentrations of each elements are calculated from these intensities using the approach outlined for Xe and the ratio of the number of sputtered neutrals inside the postionization region is known, the results should coincide with the sample composition. The results presented here provide an initial framework for acquiring quantitative elemental information. The next step in our experiments is to acquire a library of cross sections and the relative number of neutral particles in the laser beam.

The authors acknowledge the office of Naval Research and the National Science Foundation for financial support.

## References

- [1] K. F. Willey, C. L. Brummel, N. Winograd, *Chem. Phys. Lett.* **267** (1997) 359
- [2] P. Lambropoulos and X. Tang, *J. Opt. Soc. Am. B* **4** (1987) 821
- [3] F A Ilkov, J E Decker and S L Chin, *J. Phys. B At. Mol. Opt. Phys.* **25** (1992) 4005
- [4] V. P. Krainov and B. Shokri, *JETP* **80** (1995) 657
- [5] M. V. Ammosov, N. B. Delone and V. P. Krainov, *Sov. Phys. JETP* **64** (1986) 1191